

Analysis of plasma formation during hypersonic flight in the earth atmosphere

*Original*

Analysis of plasma formation during hypersonic flight in the earth atmosphere / Esposito, S., D'Ambrosio, D.. -  
ELETTRONICO. - 37:(2023), pp. 179-183. (AIDAA XXVII International Congress Padova, Italy 4-7 September , 2023)  
[10.21741/9781644902813-39].

*Availability:*

This version is available at: 11583/2985002 since: 2024-01-12T12:49:15Z

*Publisher:*

AIDAA

*Published*

DOI:10.21741/9781644902813-39

*Terms of use:*

This article is made available under terms and conditions as specified in the corresponding bibliographic description in the repository

*Publisher copyright*

(Article begins on next page)

# Analysis of plasma formation during hypersonic flight in the earth atmosphere

Salvatore Esposito<sup>1,a\*</sup>, Domenic D' Ambrosio<sup>2,b</sup>

<sup>1</sup>Dipartimento di Elettronica e Telecomunicazioni, Politecnico di Torino, Torino, Italy

<sup>2</sup>Dipartimento di Ingegneria Meccanica e Aerospaziale, Politecnico di Torino, Torino, Italy

<sup>a</sup>salvatore\_esposito@polito.it, <sup>b</sup>domenic.dambrosio@polito.it

**Keywords:** Hypersonic Aerodynamics, Plasma, Non-Equilibrium, Thermo-Chemistry

**Abstract.** In this study we investigate the formation of plasma in hypersonic flight and its impact on radio communications and radar tracking. The transfer of kinetic energy from the vehicle to the surrounding gas in the hypersonic regime leads to the formation of plasma, which can cause interference with electromagnetic waves. By conducting a numerical simulation campaign using Computational Fluid Dynamics (CFD), we are determining the critical Mach number and altitude conditions that lead to plasma formation. The plasma generated at the nose of the vehicle and its subsequent convection along the body and in the wake are the main subjects of our investigation. The simulations include physical models that account for chemical, vibrational and electron-electron energy non-equilibria, using a two-temperature approach. The results indicate the Mach numbers and altitudes at which plasma formation can significantly affect the propagation of electromagnetic waves.

## Introduction

Hypersonic flight presents a significant challenge to aircraft design and operation due to the highly complex gas flow characteristics that occur when objects travel at speeds well in excess of the speed of sound. In hypersonic flight, the transfer of kinetic energy from the object to the surrounding gas creates a region of high temperature around the body, leading to the formation of plasma [1], which can greatly affect the propagation of electromagnetic waves. If the charge density in the plasma is high enough, the wave can be completely reflected. Specifically, if the collision frequency tends to zero and the frequency of the radio link is less than or equal to the plasma frequency (satisfying the cut-off condition), the real part of the permittivity tends to zero or becomes negative. As a result, the electromagnetic wave becomes evanescent, resulting in an exponential decay of its intensity as it traverses that region of space [2]. The plasma surface thus replaces the surface of the body, distorting the reflected radiation and altering the radar trace. Even if the plasma frequency is below the cut-off values, refraction and absorption can still occur, causing a redistribution of electromagnetic waves and a reduction in re-radiation.

Understanding and predicting plasma formation around hypersonic vehicles is therefore critical for accurate tracking and evaluation of radio communication capabilities.

We present a numerical simulation campaign based on CFD tools focused on the prediction of plasma formation in suborbital hypersonic flight. The aim of the research is to determine the Mach number and altitude conditions that could produce regions around the vehicle where the plasma frequency, collision frequency (and hence permittivity) reach critical levels. For this purpose, we consider a test matrix with Mach numbers between 8 and 16 and altitudes between 20 and 70 km. We analyze the plasma formation at the nose of the vehicle and its subsequent convection along the conical nose and in the wake. We use this data to show the flight regimes in which plasma formation can interfere with the propagation of electromagnetic waves, and we superimpose this



with surface temperature data to eliminate flight conditions that are not feasible for thermal protection reasons.

### Physical Model and Numerical Method

The adopted physical model is based on the Navier-Stokes equations and includes non-equilibrium phenomena involving vibrational and electronic energy relaxation, as well as chemical and ionization reactions. We consider air as a gas mixture potentially composed of 7 chemical species, namely monoatomic oxygen and nitrogen,  $O$  and  $N$ , nitric oxide,  $NO$ , diatomic oxygen and nitrogen,  $O_2$ ,  $N_2$ , the positive ion  $NO^+$ , and electrons,  $e^-$ . The effects of non-equilibrium energy on air chemistry are represented by a two-temperature model. The rates of the chemical reactions are derived from [4,5], while the thermodynamic properties of each chemical species are taken from [6].

Due to the flight conditions, a non-magnetized, inhomogeneous, collisional cold plasma model is assumed. Under this premise, the relative permittivity,  $\epsilon_r$ , which determines the wave transmission in a medium, can be approximatively described by the Drude model [2]:

$$n^2 = \epsilon_r = 1 - \frac{(f_p e^2)}{(f(f + if_c))} = 1 - \frac{(f_{pe}^2)}{(f^2 + f_c^2)} + \frac{i(f_{pe}^2 f_c)}{(f(f^2 + f_c^2))}. \quad (1)$$

In Eq. (1),  $n$  is the refractive index at the frequency of the electromagnetic wave,  $f$ . The electron number density,  $n_e$ , determines the electron plasma frequency as in Eq. (2):

$$f_{pe} = \frac{1}{2\pi} \sqrt{e^2 n_e / \epsilon_0 m_e}. \quad (2)$$

where  $e$  is the electric charge,  $m_e$  is the effective mass of the electron, and  $\epsilon_0$  is the permittivity of free space.

The term  $f_c$  is the collision frequency between electrons and neutral particles, defined as:

$$f_c = \frac{1}{2\pi} \sum_i n_i \sigma_{i,e} \sqrt{\frac{8k_b T}{\pi m_e}}. \quad (3)$$

where  $n_i$  and  $\sigma_{i,e}$  are respectively the number density and the neutral-electron scattering cross section for the neutral species  $i$ ,  $T$  is the temperature and  $k_b$  is the Boltzmann constant.

The real part of  $\epsilon_r$  governs the wave propagation, while the imaginary part controls the collisional absorption, i.e., the transfer of energy from electrons to neutral species.

The mathematical formulation of the physical model is solved numerically using the CFD software ICFD++ by Metacomp Technologies. It utilizes a finite volume discretization approach, employing a Harten-Lax-van Leer-Contact (HLLC) approximate Riemann solver with Total Variation Diminishing (TVD) limited second-order reconstruction for the convective fluxes. The diffusive fluxes are computed using a naturally second-order centered scheme. The computational mesh is unstructured and consists primarily of polyhedral cells, except for the wall region where a structured, stretched quadrilateral grid is employed to accurately capture the boundary layer. The mesh undergoes local refinement through an Adaptive Mesh Refinement technique based on the magnitude of the Mach number gradient. The total number of cells in the mesh varies between 350,000 and 400,000, depending on the specific test case. We apply the model to an axi-symmetric blunt-nosed cone exposed to hypersonic flow. The body has an overall length of 1.125 m. The nose of the cone is an ellipsoid with minor and major radii of 2.5 cm and 5.5 cm, respectively. This is followed by a cylindrical section that is 2.5 cm long, and finally, a cone with a semi-opening angle of approximately  $8.2047^\circ$ , as described in [3]. Despite its simplicity, this geometric

configuration serves as a suitable starting point for representing plasma formation around a slender body in hypersonic atmospheric flight. To capture the plasma in the wake, the computational domain extends up to 2.875 m behind the nose.

**Results**

The results were obtained considering non-catalytic and radiation-adiabatic wall conditions, assuming a zero angle of attack to ensure axisymmetric flow. Applying a radiation-adiabatic wall boundary condition implies that the wall is considered adiabatic, but it can radiate heat received from the flow. Such a condition is known as 'radiative equilibrium.' It is assumed that the gas is fully transparent to the radiation flowing away from the wall, while the wall benefits from radiative cooling. Previous research has demonstrated that, in many scenarios, this condition provides a reasonably accurate estimate of surface temperature compared to flight data [7]. The radiative equilibrium condition states that the heat transfer into the wall is determined by the approximate relation:

$$q_w = \epsilon\sigma T_w^4 \tag{4}$$

implying that the wall will reject all heat from the flow, except for what it can radiate away. In Eq. (4),  $\sigma=5.67\times 10^{-8}$  W/m<sup>2</sup>/K<sup>4</sup> is the Stefan-Boltzmann constant, while  $\epsilon$  is the surface emissivity, which we assumed to be equal to 0.8 in this work.

The permittivity was calculated for an electromagnetic wave frequency of 1 GHz, which is typical for land-based long-range surveillance radars [8]. Setting the maximum possible temperature at the vehicle surface to 3500 K, Table 1 shows that the Mach 14 and 16 conditions at 20 km altitude and the Mach 16 condition at 30 km altitude are not feasible. The results also show that no thermochemical phenomena are observed at an altitude of 70 km for Mach numbers between 8 and 10, and therefore these observations have not been reported.

*Table 1 – Maximum wall temperature in Kelvin degrees.*

z[Km]\M	8	9	10	12	14	16
70	/	/	/	1.47E+03	1.68E+03	1841
50	1.56E+03	1.74E+03	1.91E+03	2.05E+03	2.27E+03	2.51E+03
30	2041	2.30E+03	2.43E+03	2.82E+03	3.29E+03	3761
20	2.25E+03	2.43E+03	2.83E+03	3.34E+03	3845	4.44E+03

Figures 1 to 4 indicate that along the symmetry axis in the region of the cone nose and at four different stations in the wake, the plasma frequency and the collision frequency reach their maximum values, and the real part of the permittivity reaches its minimum values. For the highest Mach numbers (at least M=12), the permittivity decreases below unity even in the wake, indicating refraction of electromagnetic waves in this region. However, significant permittivity values are only observed at altitudes of 30 and 50 km.

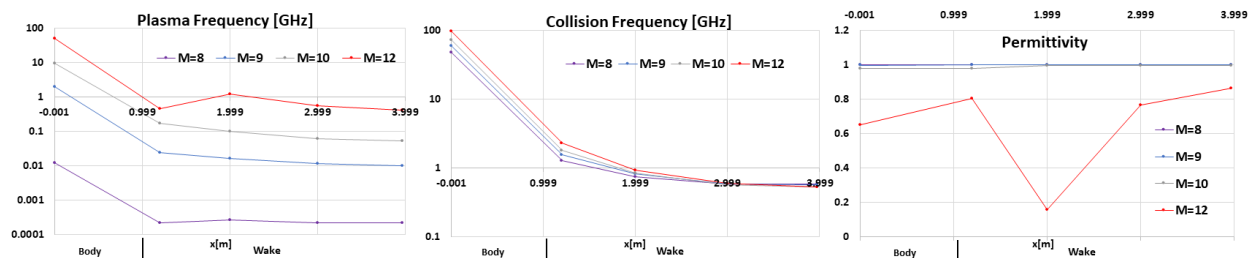


*Figure 1. Maximum plasma and collision frequencies, and minimum real part of permittivity at 20 km altitude.*

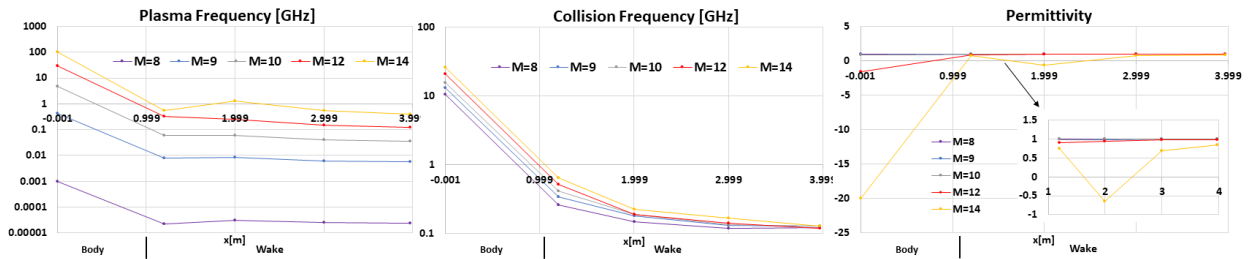


Figure 2. Maximum plasma and collision frequencies, and minimum real part of permittivity at 30 km altitude.

Specifically, the results presented in Fig. 1 indicate that the conditions at 20 km altitude correspond to highly collisional regimes with relevant collision frequencies. Significant permittivity values are observed only at Mach 12. Regarding the results in Fig. 4, the very low pressure at 70 km altitude limits the thermodynamic activity, resulting in relevant conditions only for Mach 16 and at the nose, while plasma formation in the wake remains negligible.

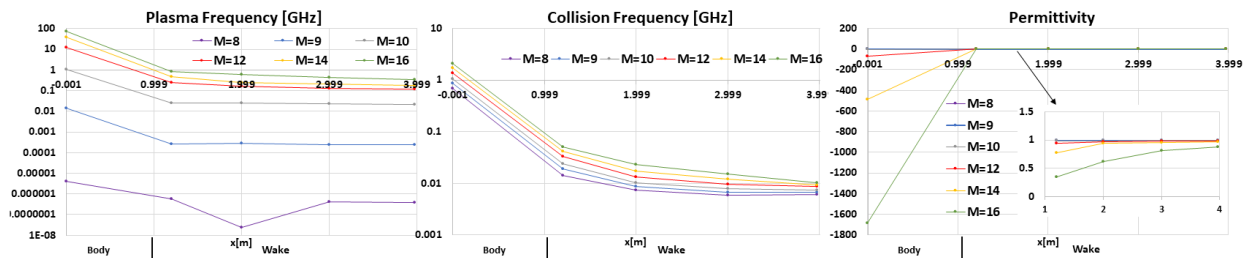


Figure 3. Maximum plasma and collision frequencies, and minimum real part of permittivity at 50 km altitude.

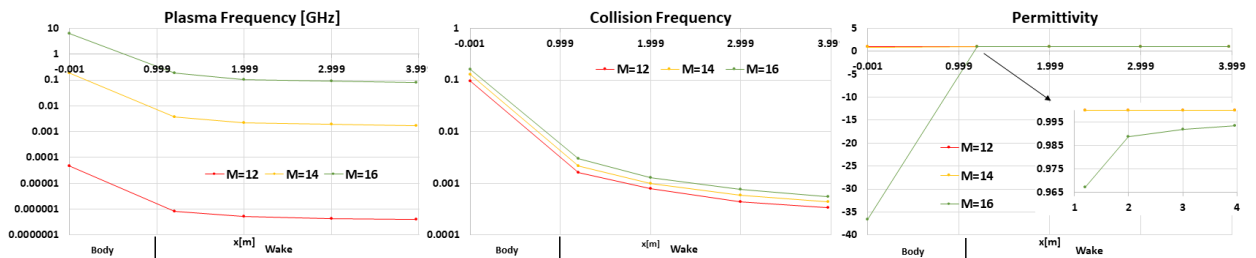


Figure 4. Maximum plasma and collision frequencies, and minimum real part of permittivity at 70 km altitude.

### Conclusions

The objective of this study was to understand plasma formation during hypersonic flight and its impact on radio communications and radar tracking using CFD tools and non-equilibrium thermochemical models. The results showed that at altitudes between 30 and 50 kilometers and Mach numbers above 12, the plasma sheath can have a significant effect on the propagation of electromagnetic waves. Subsequent research will include an analysis of the scattering of electromagnetic waves induced by the plasma, with focus on the study of the radar cross section.

### References

- [1] Anderson, John David. Hypersonic and high temperature gas dynamics. AIAA, 1989.
- [2] Stix, Thomas H. Waves in plasmas. Springer Science & Business Media, 1992.

- [3] Qian, Ji-Wei, Hai-Li Zhang, and Ming-Yao Xia. "Modelling of Electromagnetic Scattering by a Hypersonic Cone-Like Body in Near Space." *International Journal of Antennas and Propagation* 2017 (2017), Article ID 3049532. <https://doi.org/10.1155/2017/3049532>
- [4] Park, Chul. "Review of chemical-kinetic problems of future NASA missions. I - Earth entries." *Journal of Thermophysics and Heat transfer* 7(3), 1993: 385-398. <https://doi.org/10.2514/3.431>
- [5] Park, Chul, Richard L. Jaffe, and Harry Partridge. "Chemical-Kinetic Parameters of Hyperbolic Earth Entry." *Journal of Thermophysics and Heat transfer* 15(1), 2001: 76-90. <https://doi.org/10.2514/2.6582>
- [6] Gupta, Roop N., et al. "A review of reaction rates and thermodynamic and transport properties for an 11-species air model for chemical and thermal nonequilibrium calculations to 30000 K." NASA-RP-1232, 1990.
- [7] Gnoffo, Peter A., Johnston, Christopher O., and Thompson, Richard A. "Implementation of Radiation, Ablation, and Free Energy Minimization in Hypersonic Simulations." *Journal of Spacecraft and Rockets*. 47(2), 2010: 251–257. <https://doi.org/10.2514/1.44916>
- [8] Skolnik, Merrill I. Radar handbook. McGraw-Hill Education, 2008.